Proceedings of the 21st ICSMGE, Vienna, Austria, 14 – 19 June 2026. Pistrol, Adam & Schweiger (eds.)
Published by: ÖGG, Austrian Society for Geomechanics, Salzburg, Austria, ISBN 978-3-9503898-4-5
https://doi.org/10.53243/ICSMGE2026-891

Foundation design and geotechnical analysis of the Pelješac Bridge

Boštjan Pulko, Janko Logar
Faculty of Civil and Geodetic Engineering, University of Ljubljana, Slovenia, bostjan.pulko@fgg.uni-lj.si

Marjan Pipenbaher
PCE – Pipenbaher Consulting Engineers, Slovenska Bistrica, Slovenia

Gorazd Strniša
SLP d.o.o., Ljubljana, Slovenia

ABSTRACT: Officially inaugurated in 2022, the 2.4-kilometre-long Pelješac Bridge stands as a landmark infrastructure achievement in Croatia, celebrated for both its technical sophistication and its strategic geopolitical significance. Stretching across the waters of Mali Ston Bay in the Adriatic Sea, the bridge's design and construction addressed unique challenges, including deep, soft marine sediments, high seismicity, and strong regional winds. To overcome these challenges, 2-meter diameter steel piles were driven up to 128.6 meters below sea level. This paper presents the geotechnical conditions at the bridge site and the foundation design. The focus of the study is on comparing the pile bearing capacity obtained from dynamic load tests, further analysed using CAPWAP (Case Pile Wave Analysis Program), with results from numerical simulations using the finite element method (FEM). Specifically, it compares the outcomes of a 3D FEM analysis for a single pile with dynamic test results to assess both the deformation behaviour and the bearing capacity of a pile group relative to those of a single pile.

KEYWORDS: Pelješac bridge, pile foundations, pile driving analyzer, CAPWAP, finite element analysis.

1 INTRODUCTION

The Pelješac bridge is a multi-span semi-integral extradosed bridge located in Dubrovnik-Neretva County in Croatia. The bridge provides a fixed road link between the southern part of Croatia, including Dubrovnik, and the rest of the country while bypassing Bosnia and Herzegovina's short coastal stretch at Neum. The bridge spans the Mali Ston bay between Komarna on the northern mainland and the Pelješac peninsula (Figure 1). The bay is 21 km long and up to 2.2 km wide. The water depth at the bridge location is up to 28 m.

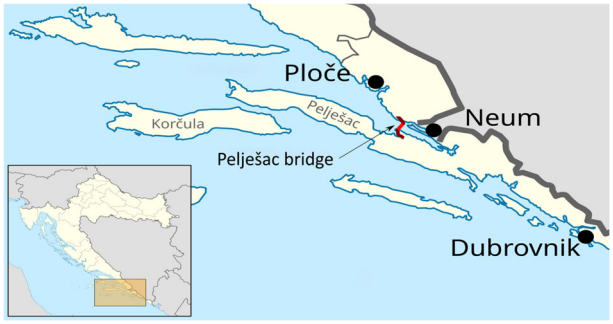

Figure 1. Pelješac bridge location (Tomobe03, 2012).

The bridge site lies in a zone of high seismicity near active faults, where seven significant earthquakes of magnitude M > 6 occurred within 100 km of the site over the past century. The site is also exposed to the extreme winds with maximum 10-minute average speeds of 33.4 m/s and wind gusts of 47.1 m/s.

2 BASIS OF BRIDGE DESIGN

The bridge has a total length of 2,404 m, is 23.6 m wide, and comprises thirteen spans, of which seven are cable-stayed - five central 285 m spans and two outer 203.5 m spans (Figure 2). The navigation channel clearance is 55 m. The pylons rise 40 m above the bridge deck. Piers at supports S5 – S10, with heights varying between 37.93 and 53.35 m, form the lower portions of the pylons. They are elastically restrained by massive pile caps positioned at the bases of the piers at sea level. Other piers S2 – S4 and S11 – S13 are between 19.2 and 31.78 m in height.

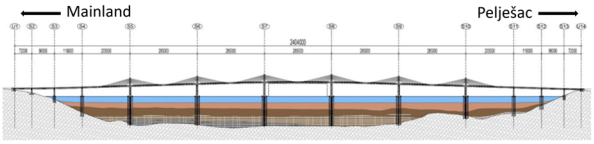

Figure 2. The longitudinal section of the Pelješac bridge.

Abutments U1 and U14, along with piers S2 and S13, are founded directly on compact rock. Piers S3 – S12, located in the sea strait, are supported by driven steel piles with diameters of 1.8 m and 2.0 m. These piles, fixed to massive concrete pile caps, range in length from 36 m to 128.6 m. At supports S3, S4, and S10 – S12, the piles are fully filled with reinforced concrete (RC) and include a RC socket for load transfer into the rock. Piers S5 – S10 are connected to massive rectangular pile caps measuring 29 × 23 m (transverse × longitudinal), with thicknesses of 4 – 5 m, and supported by 18 – 20 steel piles (2.0 m diameter, 40 mm wall thickness). All piles are end-bearing on solid rock, equipped with a 2.0 m long, 60 mm thick driving shoe. To enhance stiffness, the top 40 m of piles at piers S5 – S9 are filled with RC. The typical pier arrangement is shown in Figure 3. For more information on the bridge design, the reader is referred to Pipenbaher et al., (2019; 2022) and Pipenbaher (2023).

3 GROUND CONDITIONS

Ground conditions along the bridge alignment were determined through geological and geotechnical investigations performed between 2004 and 2011. A total of 60 boreholes, up to 130 m deep, were drilled, along with 7 CPTu tests reaching depths of 92.9 m below the seabed. Seismic data were obtained using spectral analysis of surface waves (SASW), seismic cone penetration, and the downhole method (Ivšić et al., 2009). Laboratory testing on borehole samples included standard index tests as well as oedometric, triaxial, and resonant column tests. In 2018, an additional 17 boreholes were drilled to verify bedrock depth as required by tender documentation.

Based on the geotechnical investigation results, the subsurface profile along the bridge axis was classified into four characteristic soil and rock layers, as illustrated in Figure 3:

- Zone A (0 to ~15 m below seabed): Composed of recent, very soft to soft clayey marine sediments with typical undrained shear strengths up to 25 kPa.
- Zone B (~15 to 60 m): Consists of soft to firm clays with undrained shear strength ranging from 25 to 70 kPa.
- Zone C (below ~60 m): Formed of overconsolidated and locally cemented stiff clays, transitioning beyond 75 m into a mixture of clay, sand, and gravel. Undrained shear strength ranges from 100 to 300 kPa, with an average of approximately 150 kPa.
- In the central part of the bridge, where the sea depth is about 27 m, the bedrock, composed of limestone and dolomite, lies approximately 100 m below the seabed.

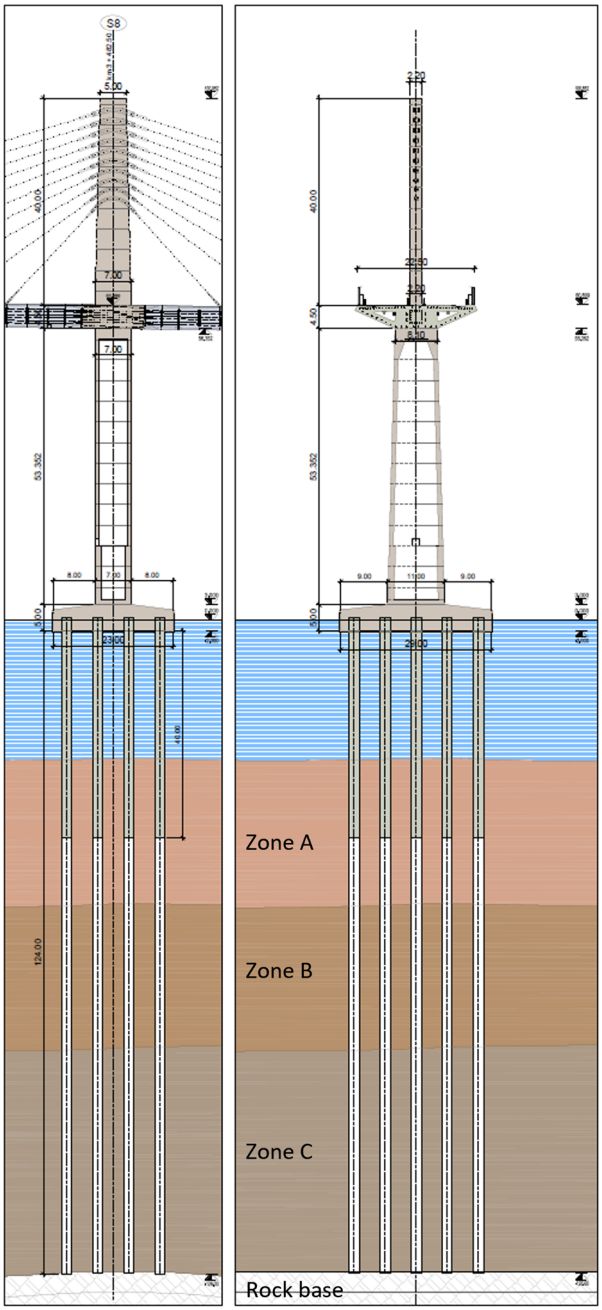

Figure 3. Typical cross section – pier S8.

Based on the collected data, the soil and rock properties were characterized using the Hardening Soil model with small-strain stiffness (HSsmall) for soils and the Hoek–Brown failure criterion for the rock mass. The HSsmall parameters adopted for the soil layers are presented in Table 1.

Table 1. Soil properties – HSsmall model.

Parameter	Unit	Zone A	Zone B	Zone C
Unit weight	kN/m^3	15.5	16.9	19.0
E_{50}^{ref}	MPa	2.0	2.5	5.0
E_{oed}^{ref}	MPa	1.5	2.0	3.5
E_{ur}^{ref}	MPa	14.0	17.5	21.0
Eff. cohesion c'	kPa	1	11	23
Eff. shear angle φ'	°	30	29	24
G_0^{ref}	MPa	55	80	95
$\gamma_{0.7}$	-	$3x10^{-4}$	$3x10^{-4}$	$3x10^{-4}$
p_{ref}	kPa	100	100	100
power (m)		1	1	1
OCR	-	1	1	2
R_{inter}	-	0.5	0.5	0.5

For the remaining soil parameters, default model values from the Plaxis 3D code were adopted. Material parameters for the bedrock are shown in Table 2.

Table 2. Rock base properties – Hoek-Brown model.

Parameter	Unit	Limestone (dolomite)
Unit weight	kN/m^3	26
Young's modulus E	GPa	55 (47)
Poisson's ratio ν	–	0.3
Intact rock strength σ_{ci}	MPa	125 (80)
Material constant m_i	–	10
Geological strength index GSI	–	50 (35)
Disturbance factor D	–	0

Material parameters were determined to evaluate pile bearing capacity, perform 3D numerical static, dynamic, and pushover analyses of the representative pier, and develop $p-y$ curves for pile-soil interaction. The geotechnical analyses of the representative pier were performed for the purpose of calibration and verification of bridge's structural model.

4 BEARING CAPACITY OF PILES

The ultimate pile shaft resistance f_s was determined from cone penetration tests (CPTu) results, in accordance with Eurocode 7-2. The average values of f_s equal to 12, 32 and 105 kPa were adopted for zones A, B and C, respectively. For the socketed piles at piers S3, S4, S10 - S12, where reinforced concrete piles are drilled into the bedrock beyond the steel piles, which were only driven down to the bedrock base, the shaft resistance f_s = 1.5 MPa was taken as a cautious estimate not exceeding 5% of the concrete compressive strength.

The characteristic uniaxial strength of the rock base generally exceeded that of the concrete (f_{ck} = 30 MPa). Therefore, for socketed piles with the diameter of 1.75 m in full contact with the rock base, the design toe bearing capacity was limited by the structural capacity of concrete.

Open-ended steel piles beneath piers S5 – S9 were only driven down to the contact with bedrock. As there are no reliable analytical expressions for determining the toe bearing capacity of open-ended, large-diameter steel piles, the pile toe bearing capacity was evaluated using nonlinear axisymmetric 2D FEM analysis (Figure 4). The analysis result for the open-ended steel pile, with an outer radius of 1 m, wall thickness of 4 cm, and a 2 m long and 60 mm thick driving shoe, is shown in Figure 4. The data from Table 2 were adopted for the bedrock with a safe estimate of uniaxial compressive strength (UCS) of the intact rock σ_{ci} = 80 MPa with GSI = 35 and GSI = 50. The steel pile was gradually loaded by imposing vertical

displacements until the numerical failure was reached (Figure 5).

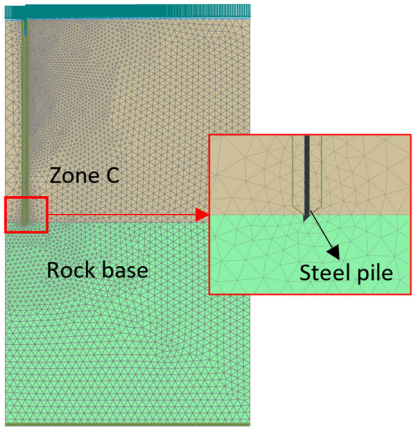

Figure 4. Finite element mesh – steel pile toe capacity.

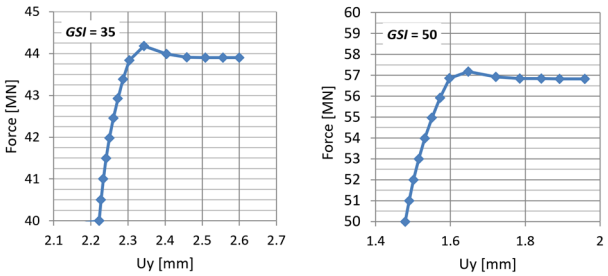

Figure 5. Load-displacement curves for *GSI* = 35 and *GSI* = 50.

The design values of pile bearing capacities in compression and tension were calculated according to Eurocode 7 based on geometry from the bridge design and shaft and toe resistances as listed above and by taking into account the specific conditions at each individual pier.

The bearing capacities of socketed piles were not critical; therefore, only the values for piers S5 – S9 are presented below. The calculated design pile capacities for piers S5 – S9 in compression and tension exceeded the design loads, ranging from 40.1 MN (S6) to 53.8 MN (S8) in compression and from 21.0 MN (S6) to 26.1 MN (S8) in tension. It should be noted that, apart from the FEM analysis of the toe capacity of the open-ended steel piles, the design pile bearing capacities were obtained using analytical methods.

5 SUPPLEMENTARY FEM ANALYSIS

During the design phase, before final geotechnical investigations were made by the contractor, shaft capacity was initially estimated conservatively using undrained shear strength derived from CPTu data. Following pile installation, high-strain dynamic testing and pile driving monitoring using a Pile Driving Analyzer (PDA) revealed that the shaft resistance in the clay layer above the rock base (Zone C) was significantly higher than initially assumed – up to twice the originally estimated value. Additional investigations and observations during pile driving confirmed that the piles at pier S6 did not reach the originally proposed limestone bedrock. Instead, they terminated in marl, which at this location forms a transitional layer between the underlying limestone and overlying clay. The quality of limestone at pier S7 was also found to be lower than initially assumed; therefore UCS was reduced to σ_{ci} = 40 MPa, and *GSI* = 35 was adopted. Additionally, Young's modulus was reduced to E = 5.5 GPa, primarily to avoid numerical instability.

Supplementary finite element analyses were performed to check the load-bearing capacity of piles at piers S6 and S7, incorporating site-specific geotechnical conditions. The analyses also aimed to compare numerical predictions with in-situ pile test results (PDA and CAPWAP) and to evaluate the effects of pile group interaction on the pier behaviour. To better align with CAPWAP results based on PDA data for pile TP7, the soil-pile interface factor R_{inter} was adjusted from 0.5 to 0.8, 0.75, and 1.0 for Zones A, B, and C, respectively. Except for these modifications reflecting actual bedrock conditions and interface properties, all other soil parameters were maintained as previously defined.

5.1 *Finite element modelling*

Two finite element setups were used: Setup A modelled a single pile, while Setup B analysed a pile group under vertical loading, incorporating plane-symmetry conditions. Figure 6 shows the FE meshes for piers S6 and S7. In Setup A (a, c), piles were modelled as open-ended steel tubes (S) or as tubes partially filled with RC in the upper 40 m (S+C) - strengthened piles. In Setup B (b, d), only strengthened piles (S+C) were considered. Interface elements were used in all models. The numerical models extend to 150 m below sea level, with piles reaching the rock layer, marl for S6 and limestone for S7, at depths of 116.1 m and 127.1 m, respectively. Model dimensions are 15 × 15 m for Setup A and 58 × 46 m for Setup B. Drained conditions were assumed.

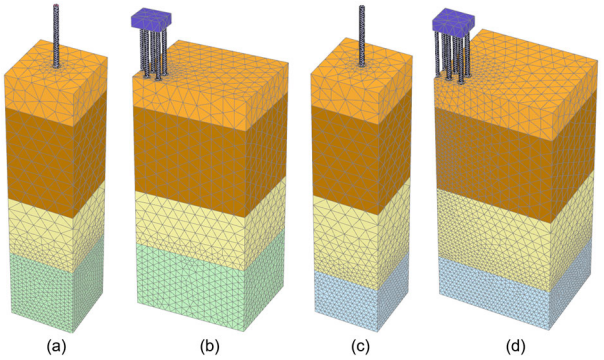

Figure 6. FE setups for piers S6 (a, b) and S7 (c, d).

5.2 *Pile TP7 (S7) – comparison with CAPWAP analysis*

To validate the numerical model, a finite element (FE) analysis was performed on steel pile TP7 at pier S7 under a vertical load of 54 MN. Results were compared with CAPWAP analysis of PDA measurements taken 19 days after installation, focusing on axial force distribution along the pile (Figure 7) and load-displacement behaviour (Figure 8).

As shown in Figure 7, the axial force distribution closely matches the CAPWAP results. Shaft resistance is minimal from the seabed (27 m BSL) to about 40 m BSL, then gradually increases down to approximately 90 m BSL. A pronounced increase of shaft resistance occurs between 90 m and 102 m BSL (Zone C), followed by marked reduction in axial force down to 110 m BSL, where shaft resistance decreases because of small pile displacements.

The load-displacement curves obtained with FE and CAPWAP analyses are shown in Figure 8, demonstrating good agreement: the FE results exhibit slightly larger settlements but less nonlinearity. Based on these results, it can be concluded that the numerical model is capable of providing credible predictions of individual pile behaviour and can be applied to analyse a pile group.

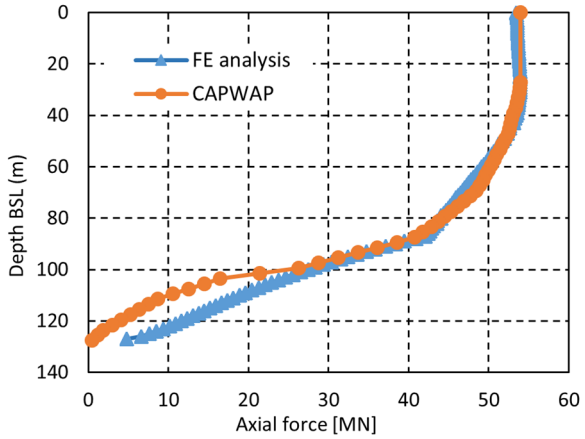

Figure 7. Pile TP7 – axial force distribution at 54 MN.

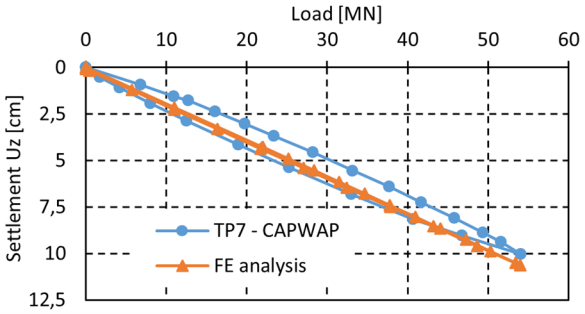

Figure 8. Load displacement curves (FEM analysis vs. CAPWAP).

5.3 *Pile group behaviour*

Assessing pile group effects is challenging due to load redistribution among piles. To evaluate their impact on displacement and bearing capacity, uniform displacements (up to 28 cm) were applied to a single pile and a pile group, with vertical reactions F_z normalized per pile for direct comparison.

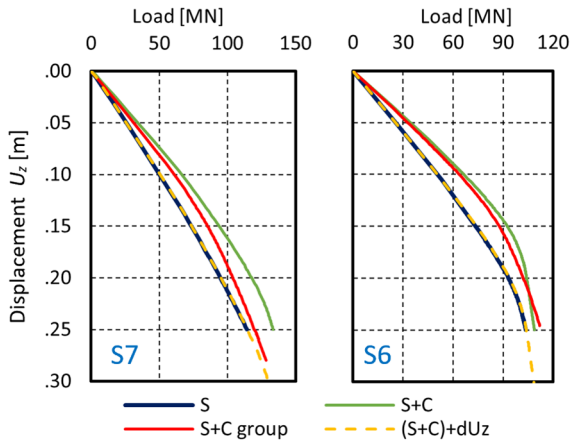

Figure 9. Load-displacement curves for single pile and pile in a group.

Figure 9 shows the load-displacement curves for piers S6 and S7. The strengthened pile (S+C) exhibits reduced displacements compared with the single steel pile (S), primarily due to the increased stiffness provided by the RC infill; no difference in shaft resistance was observed. When the elastic displacement component dU_Z, arising from the stiffness difference between the strengthened and the hollow steel pile, is added to the displacements of the strengthened pile, the results closely match those of the steel pile ((S+C)+$dU_Z \approx$ S).This indicates that the RC plug has a negligible influence on the vertical load transfer and overall bearing capacity.

The influence of the pile group on displacements is relatively small. Under identical loading, the pile group exhibits somewhat higher displacements than the single pile. The average displacement group factor under working loads up to 80 MN per pile is approximately $\alpha = U_{Z,group}/U_{z,1} = 1.06$ for pier S6 and $\alpha = 1.12$ for pier S7. The group effect on overall bearing capacity of the piles is negligible.

6 CONCLUSIONS

The foundation design of the Pelješac Bridge (Figure 10) represented both a unique challenge and an opportunity to apply various approaches and techniques in design, pile testing, and result analysis.

Figure 10. Pelješac bridge.

Through the process, we found that:

- High-quality geotechnical investigations are essential for the successful execution of demanding projects.
- Combining established analytical methods with advanced numerical techniques, supported by sound engineering judgment, proves effective in the design process.
- In-situ pile load testing is crucial for verifying bearing capacity and predicting displacements.
- The design pile bearing capacity values derived from numerical and analytical calculations were sufficiently conservative, preventing issues during bridge construction.
- The calculated pile behaviour corresponds well with that obtained from the CAPWAP analysis.
- Well-designed numerical models enable credible predictions of the behaviour of individual piles and pile groups.
- The analysis of both single piles and pile groups indicated a relatively small group effect on settlements and a negligible impact on bearing capacity.

7 REFERENCES

Ivšić, T., Vrkljan, I., Zlatovic, S. and Mavar, R., 2009. Dynamic testing of marine sediments at the Pelješac bridge site. https://doi.org/10.3233/978-1-60750-031-5-344.

Pipenbaher, M., 2023. Pelješac bridge, Croatia – Part 1: Concept and Design/Pelješac-Brücke, Kroatien – Teil 1: Konzept und Planung. *Bauingenieur*, 98(05), pp.147–155. https://doi.org/10.37544/0005-6650-2023-05-39.

Pipenbaher, M., Hrelja Kovacevic, G., Petersic, T. and Mujkanovic, N., 2019. Pelješac bridge – design and maintenance. In: *Future Trends in Civil Engineering*. [online] Future Trends in Civil Engineering 2019. University of Zagreb Faculty of Civil Engineering. pp.219–240. https://doi.org/10.5592/co/ftce.2019.10.

Pipenbaher, M., Peteršič, T., Mujkanović, N., Hrelja Kovačević, G. and Trogrlić, Z., 2022. Pelješac bridge - Design and construction. In: *IABSE Reports*. [online] IABSE Symposium, Prague 2022: Challenges for Existing and Oncoming Structures. Prague, Czech Republic: International Association for Bridge and Structural Engineering (IABSE). pp.670–677. https://doi.org/10.2749/prague.2022.0670.

Tomobe03, 2012. *English: location map of Neum strip (red), dividing territory of the Republic of Croatia around Dubrovnik from the rest of Croatia*. Available at: <https://commons.wikimedia.org/wiki/File:Neum_strip_location_map.svg#Licensing> [Accessed 15 July 2025].